IEEE Photonics Journal
An IEEE Photonics Society Publication

Open Access

The Optimization Design of Sub-Regions Scanning and Vibration Analysis for Beaconless Spatial Acquisition in the Inter-Satellite Laser Communication System

Volume 10, Number 6, December 2018

Yunjie Teng
Min Zhang
Shoufeng Tong

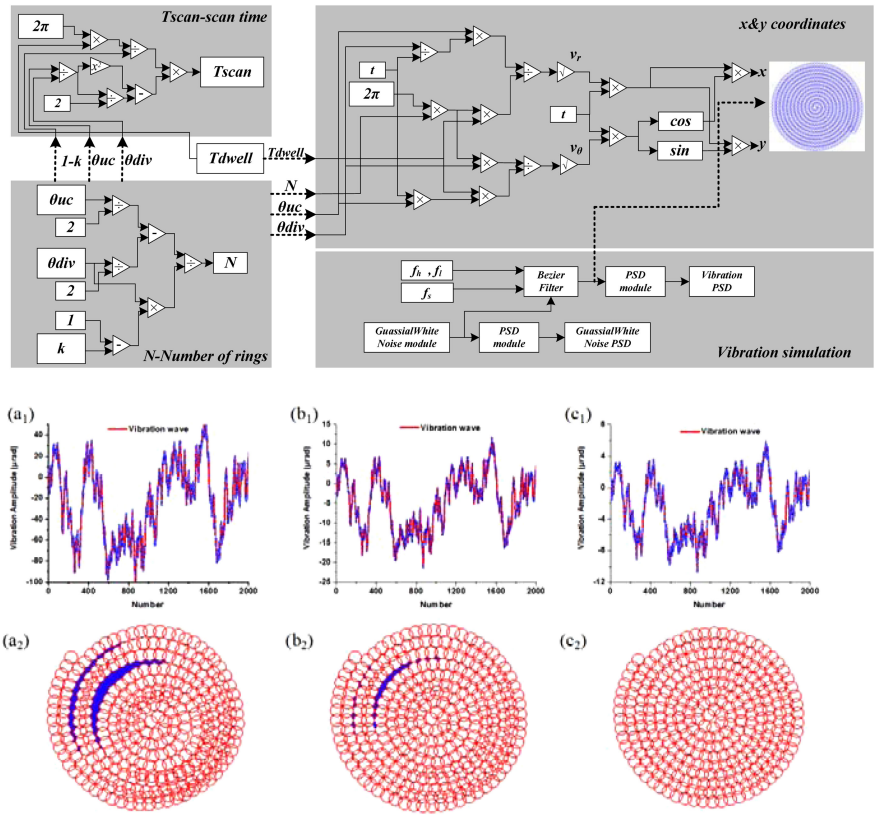

DOI: 10.1109/JPHOT.2018.2884718

The Optimization Design of Sub-Regions Scanning and Vibration Analysis for Beaconless Spatial Acquisition in the Inter-Satellite Laser Communication System

Yunjie Teng,[1, 2] **Min Zhang,**[2] **and Shoufeng Tong**[2]

[1]School of Opto-Electronic Engineering, Changchun University of Science and Technology, Changchun 130033, China
[2]Institute of Space Optoelectronics Technology, Changchun University of Science and Technology, Changchun 130033, China

DOI:10.1109/JPHOT.2018.2884718

Manuscript received October 25, 2018; revised November 27, 2018; accepted November 29, 2018. Date of publication December 3, 2018; date of current version December 13, 2018. Corresponding author: Min Zhang (e-mail: 1297891415@qq.com).

Abstract: We mainly report an efficient approach to optimize the design of beaconless spatial laser acquisition. In order to analyze the influence of vibration environment on the beaconless spatial acquisition, a demonstration of an efficient method will be presented to simulate the level of satellite platform vibration. An important power spectral density (PSD) model of satellite platform vibration used by the European Space Agency is introduced. Then through LABVIEW, a simulated vibration waveform is generated, and the simulated PSD has a basic consistency with the in-orbit measurement spectral line, referring to the design of the filter, generating the Gaussian white noise sequence, filtering the pseudorandom signal and the whole processing procedure of parameter matching. The variation interval of the vibration amplitude is from -100 to 40 μrad. Then, the model of beaconless acquisition is proposed, which uses the spiral scan pattern, laser with a divergence angle of 80 μrad scan in an uncertainty cone (UC), and also the scan coupled with the simulated vibration is given. Through the beaconless acquisition program, the vibration is suppressed between -10.7 and 5.9 μrad; when the overlap factor is selected as 10%, it does not produce any leakage scanning area. It can be used for a wide variety of platforms. This new method will be good for analysis and test of beaconless spatial acquisition algorithm. Finally, the description of acquisition duration, which mainly includes the fast steering mirror spiral scan and the mechanical rotary table step scan, is introduced. And the corresponding optimal selection method of sub-region is proposed; the design of 1.6-mrad scanning pattern with 7×7 sub-regions in the 8-mrad acquisition UC is given. Through the actual measurement, the acquisition time is 18.21 s, the tracking error is better than 0.4 μrad.

Index Terms: Beaconless spatial acquisition, laser communication, satellite vibration, power spectral density, spiral scan.

1. Introduction

Laser is a carrier of information in the satellite optical communication system. In order to build and maintain a stable laser link, a set of high-precision pointing, acquisition and tracking system must be established because of the narrow beam width and long transmission distance.

For the satellite optical communication system, the beaconless spatial acquisition is required between the laser communication terminals. Compared with the typical acquisition process, beaconless algorithm investigates the elimination of beacon laser, instead of using the narrow divergence communication beam for acquisition [1]–[3], the spiral scanning mode of laser beam is used in the uncertain areas. In the acquisition process of laser link, the vibration and attitude change of the satellite platform will affect the laser beam acquisition probability. The communication terminal relies on a precision laser beam pointing, acquisition and tracking, so for the acquisition process, a detailed research and analysis of the influence factors such as satellite platform vibration are needed for a proper design [4]–[7]. The first in orbit measurements of Landsat-4 dynamic disturbances were published in 1984 [8]. Another analytical investigation about the influence of vibrations is presented in [9]–[12]. Japan's NASDA used satellite-based laser link experimental satellite ETS-VI to conduct a vibration measurement. According to the in-orbit test results, the power spectral density of the measurement results is shown as follows, between the frequency ranges from 0.39 Hz to 250 Hz, the mean square deviation of the vibration amplitude is 16.3 μrad, and most of the frequencies are less than 100 Hz. According to the FSM deflection angle of fine tracking, the micro-oscillation will be get. When the sampling frequency is 500 Hz, the mean square deviation of the vibration is 5.13 μrad in the azimuth axis and 7.30 μrad in the elevation axis. When the sampling frequency is 100 Hz, the mean square deviation of the vibration is 11.2 μrad in the azimuth axis and 18.6 μrad in the elevation axis. To know the vibration level of the satellite platform is important for the parameters design of the laser beam acquisition algorithm. However, how to simulate the satellite vibration and how to achieve the analysis for the influence of vibration on the beaconless acquisition process is an important technology [13]–[16]. The reference [20] presents the result of beaconless spatial acquisitions, the scanning duration is 33.5 s, in reference [26], the experimental results of tracking precision is given for laser communication system, and the coarse and fine tracking errors are 49.1 μrad and 4.6 μrad, respectively.

Researchers have done a lot of effort to test the vibration of satellite platform, and established a theory analysis for beaconless capture algorithm. But no one give a combination for these two studies in the actual engineering application, such as the correlation analysis for the selection of the maximum vibration amplitude which based on the no leakage beaconless acquisition with a certain overlap region, this article will focus on this content.

In this paper, we use the LABVIEW software for simulation, A filter program is proposed for the first time. The filtered result approximates to the ESA's test PSD, and this program also has a universal applicability. The filter program is applied to the analysis of beaconless acquisition process for the first time, the different vibration amplitude of the satellite platform is simulated by this filter program. Adding it to a beaconless simulation program and several scanning trajectory with different vibration amplitudes are given. Then the relationship between the vibration amplitude and the scanning coverage is analyzed, when the vibration is within -10.7 μrad to 5.9 μrad, no leakage will happen during the beaconless scanning. The scanning scope of galvanometer is usually small and not enough to cover the whole UC. Therefore, a new sub-regional spiral scanning method for FSM and turntable is proposed. This kind of sub-regional composite scanning is a good solution to the limits of actuator scope.

2. PSD of the Satellite Platform Vibration

Vibration of the satellite is the platform vibration of the satellite optical communication terminal. The impact will be superimposed on the output of the tracking system. It is necessary to consider the influence in the laser beam scanning process.

The vibration characteristic of the satellite platform mainly depend on the system design [17], however, for the inter-satellite laser communication system, the magnitude and frequency of satellite vibration should meet the optical system requirement of the communication terminal. Two representative power spectra which are used separately by ESA and NASDA are discussed in [13]. The PSDs are the results of the spatial experiments which have been done by ESA and NASDA respectively. By comparison, the vibration power spectrum for the two satellites are similar. Here,

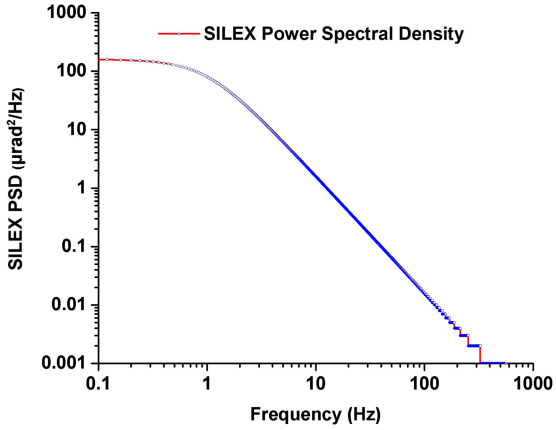

Fig. 1. Power spectral density of the satellite platform vibration.

we mainly refer to an important PSD model of satellite platform vibration, as shown in Eq. (1). [9]

$$S(f) = \frac{160\,\mu\text{rad}^2/\text{ Hz}}{1 + (f/1\ \text{Hz})^2} \tag{1}$$

The vibration of the satellite platform can be simulated effectively during ground simulation analysis. So, in this paper, the power spectrum of ESA is used to simulate the satellite platform vibration. On ESA's large communication satellite, accelerometer are installed to get measurements of the vibration levels before launch. The range of the sensor is $\pm$100 mg with a resolution of 5 μg. The measurement process is performed by measuring the displacement using differential capacitors, the measurement bandwidth is from 0.5 Hz to 1 K Hz [18].

The spectrum line is shown in Fig. 1. It can be applied for the angular motion, and has a value around 16 μrad rms. This model is often cited in many references. And the characteristic of the power spectra is its high power in low frequency area and low power in high frequency area [13]. Most of the power appears at the lower frequencies below 10 Hz.

3. Procedure of the New Method

For the simulation verification of satellite optical communication system, how to simulate the vibration of a satellite platform is an important technology. In order to analyze the influence of vibration environment on the beaconless spatial acquisition, a new method will be presented to simulate the level of satellite platform vibration. The principle of this novel approach is that the PSD of the simulated vibration waveform will have a basic consistency with the in-orbit measurement spectral line, as shown in Fig. 1. The mathematical processing method includes the design of the filter, generating the Gaussian white noise sequence, filtering the pseudo-random signal and the whole processing procedure of parameter matching. We have designed a filter program through LABVIEW. Because LBVIEW program is difficult to understand, I have replaced him with a block diagram, and the block diagram is shown as Fig. 2.

The pseudo-random signal of Gaussian distribution is generated, and the statistical distribution is (0, s), s stands for the standard deviation and its value is 800. The generated Gaussian white noise signal is shown in Fig. 3(a). And Fig. 3(b) is the corresponding PSD of Fig. 3(a).

The Gaussian white noise sequence is then filtered by a designed Bessel filter, which generates the vibration signal of the satellite platform as shown in Fig. 3(c). The type of Bessel filter is set to a low pass filter. The sampling frequency is 3 KHz. The low cutoff frequency and high cutoff frequency are 0.1 Hz and 1 K Hz, respectively. It can be seen that the variation interval of the vibration amplitude is from -100 μrad to 40 μrad.

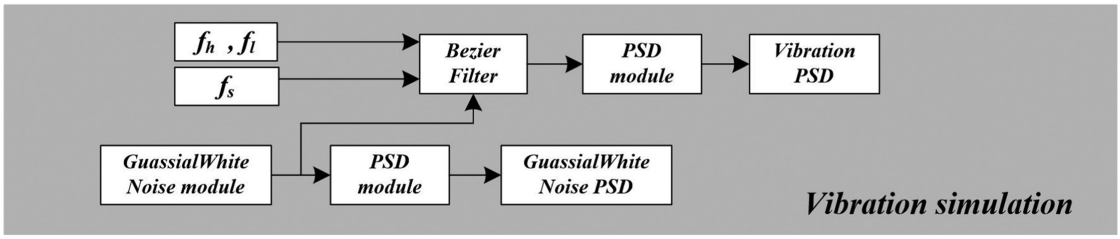

Fig. 2. LABVIEW vibration filter diagram.

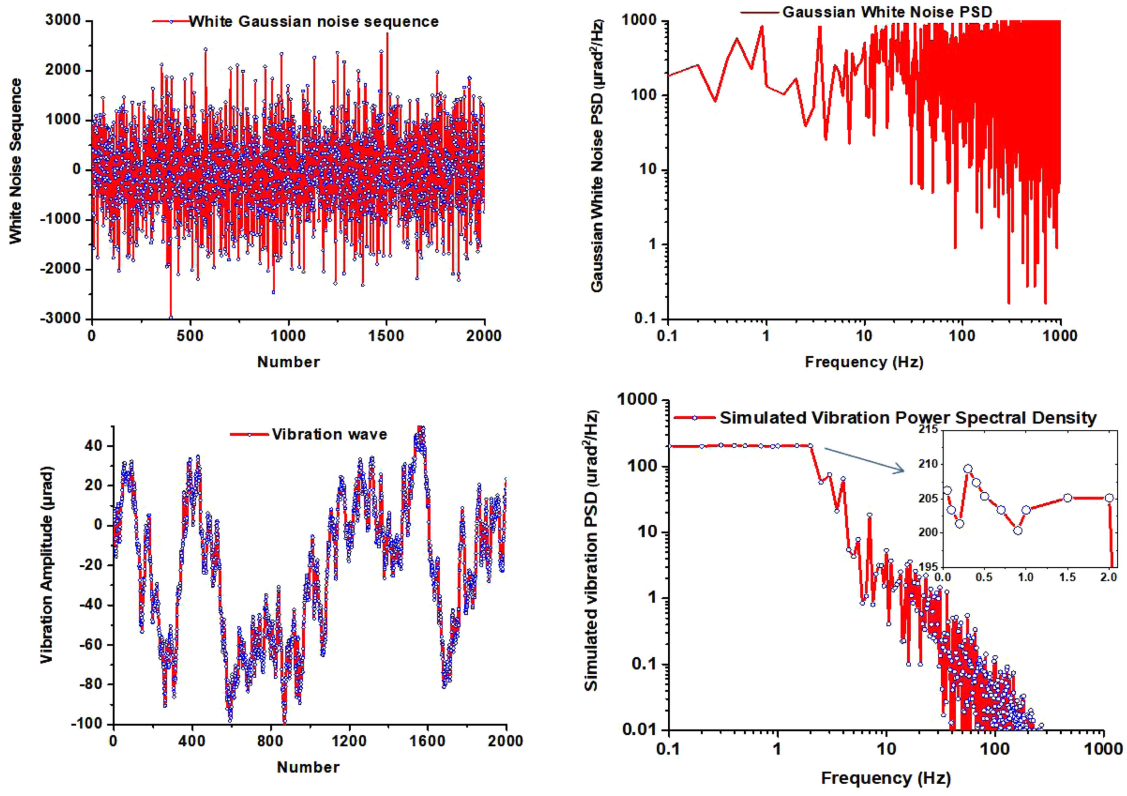

Fig. 3. The vibration of satellite platform simulated by filtering. (a) Gaussian white noise sequence. (b) Power spectral density of Gaussian white noise. (c) Satellite vibration simulation data. (d) Power spectral density of the simulated satellite vibration data.

The satellite vibration data which is simulated by a filtered Gaussian white noise is shown in Fig. 3(c). The total PSD obtained from Fig. 3(c) is shown in Fig. 3(d). Compared with Fig. 1, the PSD obtained in this method is consistent with the spectrum model which is used by ESA in the optical communication payload SILEX.

The frequency range of the PSD showed in Fig. 3(d) are from 0.1 to 1000 Hz. The amplitude is 200 μrad^2/ Hz at the low frequency range. The spectrum drops at 2 Hz, and with the frequency increases, the amplitude decreases gradually. It can be seen that the vibration amplitude is very small at the high frequency region. This indicates that the low frequency vibration is the main factor influencing the system performance of inter-satellite laser communication. We need to use Fig. 3(d) to simulate the power spectrum of the satellite platform vibration. The simulated vibration waveform shown in Fig. 3(c) can be used to analyze the following laser spiral scanning of beaconless spatial acquisition process.

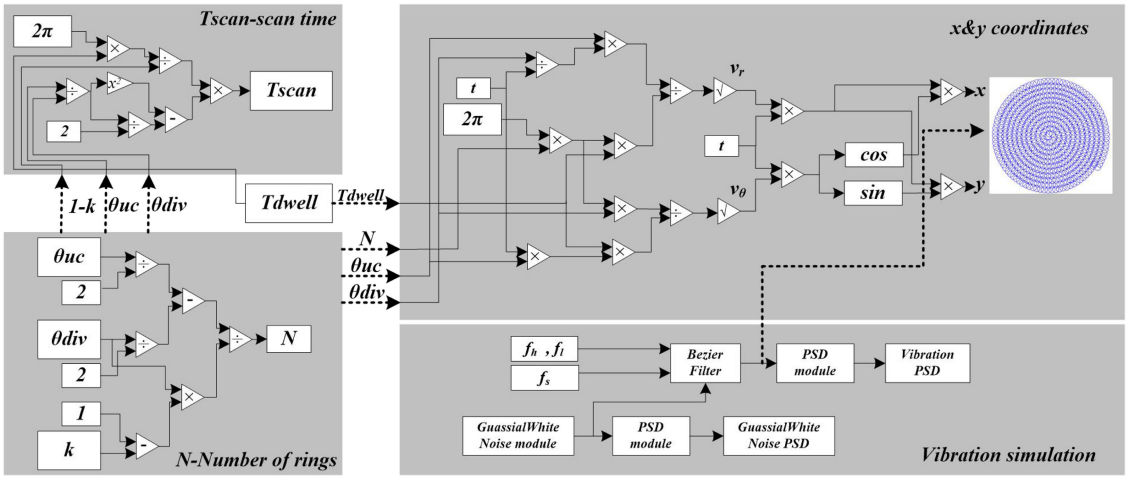

Fig. 4. LABVIEW beaconless simulation diagram.

4. Sub-Regions Scanning and Vibration Analysis for Beaconless Spatial Acquisition

4.1 Analysis for Spiral Scan With Vibration

For the inter-satellite laser communication, generally, a narrow band laser is used in the scanning and acquisition process, its main feature is to use the transmitting terminal to perform laser beam scanning, and the receive end can realize the gaze capture through the larger detection field. The transmitter uses a narrow band laser to scan the uncertain area, and linear spiral scan is a kind of commonly used laser beam search pattern, it scans the UC based on the trajectory of spiral, because the scanning begins from the center location of highest probability area to the least likely location, and each spot will dwell on the detect sensor for a constant duration, so the spiral patterns can implement a very high efficiency of acquisition [19]–[25].

Based on the center of the scanning range, the displacement of the two directions of the azimuth and elevation is the coordinate axis, and the plane rectangular coordinate system will be established. The scan range in both direction is $\pm\theta_{uc}/2$, the corresponding radial and angular scanning speed can be expressed as Eq. (2) and Eq. (3): [2]

$$V_r = \sqrt{\frac{(1-k)\,\theta_{uc}\theta_{div}^2}{2\pi t\,(\theta_{uc}-\theta_{div})\,T_{dwell}}} \tag{2}$$

$$V_\theta = \sqrt{\frac{2\pi\,(\theta_{uc}-\theta_{div})}{(1-k)\,\theta_{uc} t T_{dwell}}} \tag{3}$$

Here, θ_{uc} is the uncertain area, θ_{div} represents the laser divergence beamwidth, k is the laser overlap factor, T_{dwell} is the expression for the laser dwell time on the detector cell.

The coordinates of the trajectories of the laser movement in the two dimensional coordinate system are defined as X and Y. The laser spot coordinates are related to the velocity changes of the spiral scan as shown in Eq. (2) and Eq. (3), the relationship between them can be described by the following Eq. (4) and Eq. (5):

$$X = V_r t \cos(V_\theta t) \tag{4}$$

$$Y = V_r t \sin(V_\theta t) \tag{5}$$

We have done the beaconless scanning through the LABVIEW software. I have used the block diagrams replace LabVIEW. The block diagrams is shown as Fig. 4.

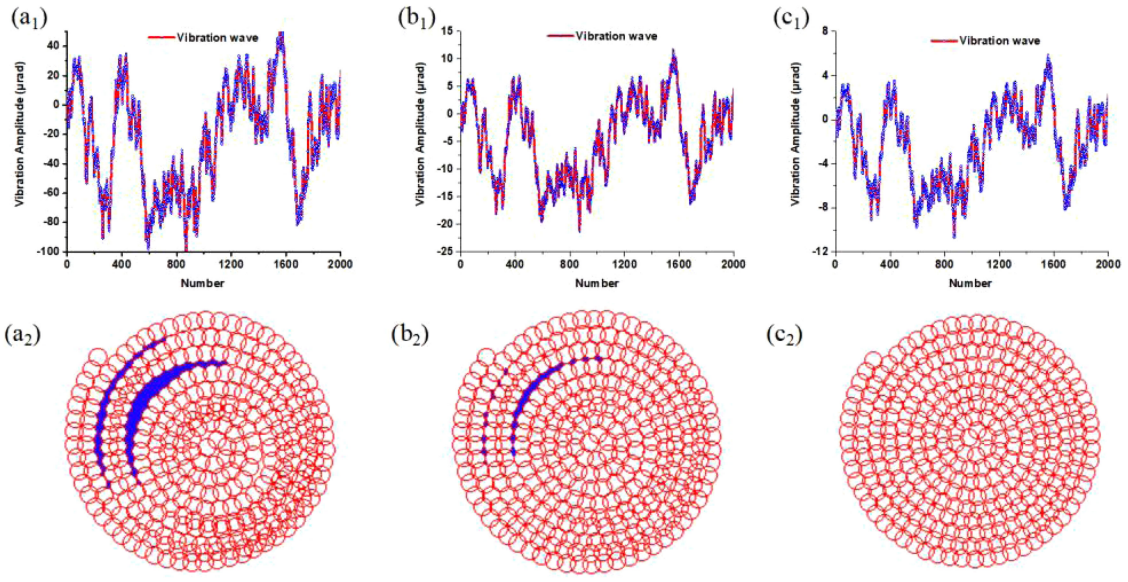

Fig. 5. Vibration analysis for beaconless spatial acquisition. (a1) Vibration data from -100 μrad to 40 μrad. (a2) Spiral scan based on vibration in (a1). (b1) Vibration data from -21.4 μrad to 11.7 μrad. (b2) Spiral scan based on vibration in (b1). (c1) Vibration data from -10.7 μrad to 5.9 μrad. (c2) Spiral scan based on vibration in (c1).

Reference [9] gives a detail description about the selection of the overlapping area, finally a 10% overlap factor is set for beaconless acquisition in the case of no vibration. The laser spot achieves a good coverage in the target area, this scanning mode doesn't consist of leakage cone, and can realize a high probability of spatial acquisition.

But for the actual acquisition process, vibration is unavoidable, and it will have a great impact on the beaconless acquisition. Next, we will add the vibration of the above simulation to the beaconless program, and the analysis will focus on the influence of vibration. Through the program written in LABVIEW, also based on the same frequency of vibration spectrum, we have tested the trajectory diagram of missing sweep area under different vibration amplitudes in the beaconless simulation. In this simulation, the laser divergence angle of 80 μrad is used to scan the uncertain area of 2 mrad.

Firstly, we choose the vibration range from -100 μrad to 40 μrad, as shown in Fig. 5(a1), add it to a beaconless acquisition program, we can see that the spiral scan has produced a very large missing scan area, the blue region for marking as shown in Fig. 5(a2), This scanning missing area is very large, and it has an non-negligible and important influence on the acquisition process of inter-satellite laser communication. We therefore procedures to reduce the vibration amplitude, the amplitude is controlled between -21.4 μrad and 11.7 μrad, as shown in Fig. 5(b1), we add this vibration to beaconless acquisition program, the scanning result is shown in Fig. 5(b2), the blue leakage scanning area is smaller than the analysis result in Fig. 5(a2). It has a significant improvement for the acquisition success probability. So the amplitude of vibration is controlled between -10.7 μrad to 5.9 μrad, as shown in Fig. 5(c1), the vibration is added into the beaconless program, as shown in Fig. 5(c2), it does not produce any leakage scanning area.

4.2 Scanning Duration and the Sub-Regions Selection

According to the previous analysis, the acquisition probability is higher in the central part of the UC, and is lower in the edge part. The laser spiral scan starts from the point of higher capture probability. The S-330.2SL produced by PI company, it is a high-dynamics piezo tip/tilt platform for fast steering mirror, the tip/tilt angle for the S-330.2SL is 2 mrad. S-330.2SL is selected for laser

spiral scan acquisition in engineering, but the UC is 8 mrad which is larger than 2 mrad. In this case, the single spiral scan pattern is not feasible. The signal laser light should scan in the whole UC to cover the optical communication terminals of the target satellite, in order to establish the optical communication link. Combined with the sub-regions spiral scan, the adjacent sub-regions will be scanned by the mechanical rotary table in step mode.

The acquisition duration is associated with the dwell time, laser divergence, scan times and the selection of overlap factors. The main components of the capture time include the FSM spiral and the mechanical rotary table stepping scan time. And the expression of acquisition time can be determined respectively as Eq. (6) and Eq. (7)

$$T_{spiral} = \frac{\pi T_{dwell}}{2(1-k)}\left[\left(\frac{\theta_{sub}}{\theta_{div}}\right)^2 - \frac{\theta_{sub}}{\theta_{div}}\right] \times N_{scan} \tag{6}$$

$$T_{step} = 3\sqrt{\frac{(1-k)\theta_{sub}}{2a}} \times N_{scan} \tag{7}$$

Here, the step scan time is associated with the bandwidth of the actuator, θ_{sub} is the sub-regions size, N_{scan} is the performed times of laser spiral scan mode, simultaneously, T_{step} is the stepping times. It can be expressed as

$$N_{scan} = \left(\frac{\theta_{uc}}{(1-k)\theta_{sub}}\right)^2 - 1 \tag{8}$$

Considering the laser transmission time at a certain communication distance, and the response time of the acquisition sensor in the receiving end. The total acquisition duration can be determined as

$$T_{total} = \left(\frac{2L}{c} + 3\sqrt{\frac{(1-k)\theta_{sub}}{2a}} + t_{res}\right)\left[\left(\frac{\theta_{uc}}{(1-k)\theta_{sub}}\right)^2 - 1\right] + T_{scan} \tag{9}$$

Here, L is the laser communication distance, c is the speed of light (3.0e + 8 m/s), a is the maximum acceleration of the mechanical rotary table, tres is the response time of the acquisition detector.

In this system, the UC is 8 mrad, the communication distance is set as 5000 km, the laser divergence beamwidth is 80 μrad, the maximum executive scope for FSM is 2 mrad, a 10% of laser spot overlap is selected [9], the response time of the acquisition detector is 10ms, for the mechanical rotary table, the maximum angular acceleration is designed as 0.696rad/s2. Depending on the formula 9, we can get the relationship between total scanning time and the different selection of sub-region size, as shown in Fig. 6.

Germans use spiral scanning, Because its uncertain area is 500–1000 urad. Fast steering mirror's effective implementation scope can cover uncertain areas. The selection of sub-regions is restricted by the scanning range of the actuator, in this paper, the UC is 8 mrad, the principle of sub-regions selection need to refer the effective implementation scope of the actuator, the executive scope for S-330.2SL is 2 mrad, considering a certain amount of residual, and combined with Fig. 6, the optimal sub-region will be designed as 1.6 mrad. The amplitude from -10.7 μrad to 5.9 μrad is added to the simulation, through simulation, the UC is divided into 7 $\times$ 7 scanning sub-regions to achieve the coverage of the acquisition uncertain region.Scanning the whole UC requires 17.86s. Based on the optimization of sub-regional selection, the scanning pattern with sub-regions in the acquisition process is shown in Fig. 7.

5. Experimental Verification

To prove the foregoing simulation, indoor environment is established in this paper. Based on periscope circumferential structure which has beaconless receiving, the experiment is mainly about (shown in the above Fig. 8): a 1550 nm near-infrared goes through 10 meters straight ray tube to

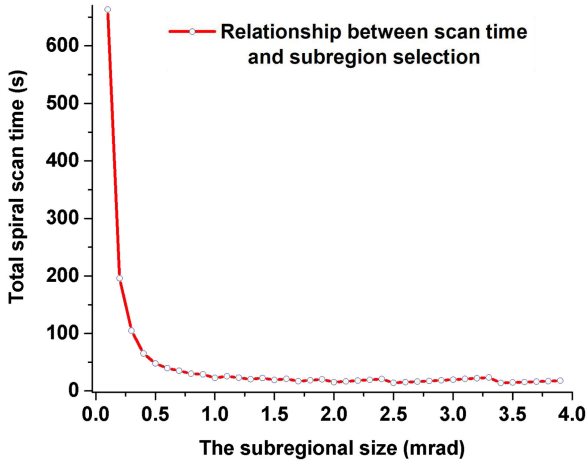

Fig. 6. Relationship between total scanning time and the different selection of subregional size.

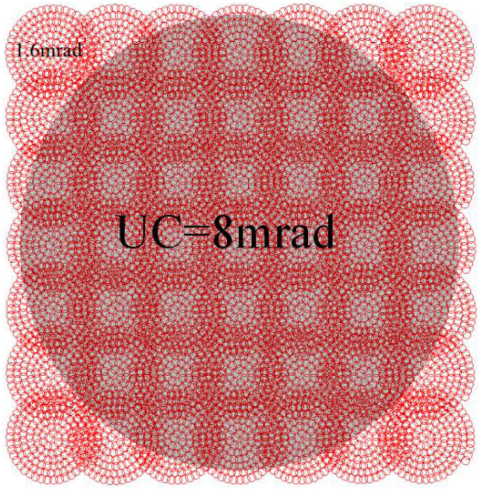

Fig. 7. Spiral scan pattern for UC coverage with sub-regions.

(a) (b)

Fig. 8. Experimental equipment (a), (b).

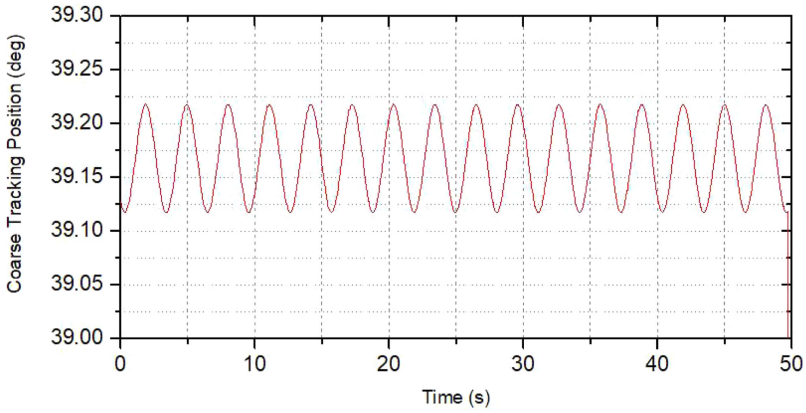

Fig. 9. 0.1 nusoidal motion.

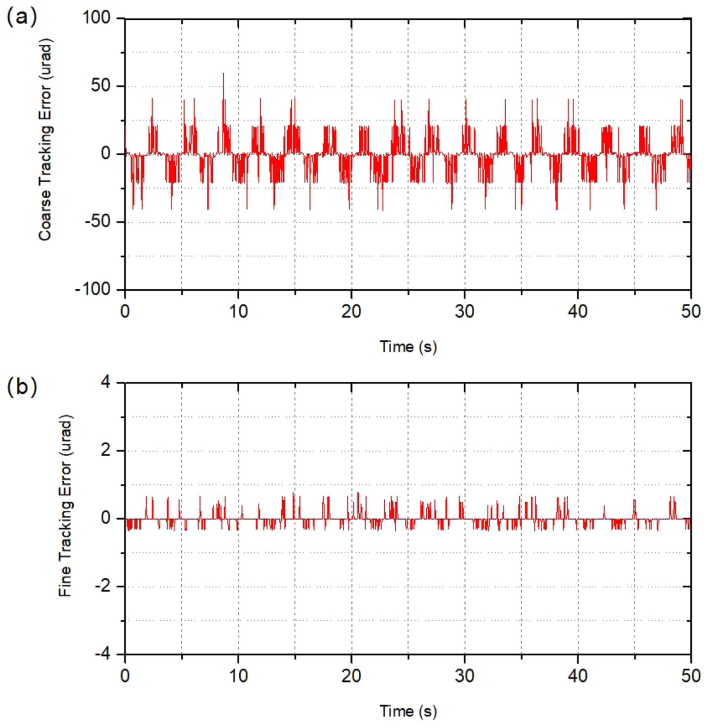

Fig. 10. (a) Coarse tracking error. (b) Fine tracking error.

simulate lighting to receiver at an infinite distance. It is a 2-D simulation platform below the periscope circumferential structure. This platform is used to simulate vibration of nusoidal motion with a period of 6.5 s and a peak of 0.1 degrees.The trajectory is shown in Fig. 9. The beam diverging angle used in this experiment is 80 μrad, the view field of monitor is 8 mrad and the overlapping region of beam mentioned in the foregoing text is 10%, which uses $7 * 7$ subarea scanning and whose many results of scanning time was better than 18.21 s. As shown in Fig. 10. Coarse tracking error are better than 40 urad, fine tracking error are better than 0.4 urad, 0.4urad belong to -10.7 μrad to 5.9 μrad. which fulfills the requirement of satellite borne laser communication. we proposed filtering method is based on the vibration power spectrum of ESA. In fact, this method is universal and can be applied to vibration power spectra of satellites of any organization. In order to reduce the load

weight and transmit power of future LEO satellites, most of the laser communication systems will adopt beaconless acquisition method. Because of the technical difficulties of beaconless acquisition technology, the selection of overlapping coverage area, acquisition time and the success of acquisition should be considered.This method can be used for detailed analysis of vibration caused leakage scanning only by simulation. To help beaconless communication systems in the early research, in overlapping areas, platform vibration suppression and acquisition time between the three to achieve an optimal choice. This experimental show that the tracking accuracy can be satisfy on satellite-to-satellite by this method when the vibration of the platform is basically the same as the above simulation.The scanning time in the experiment the same as in the simulation.

6. Conclusion

In this paper, the vibration is added to the beaconless acquisition simulation based on the LABVIEW for the first time. In the LABVIEW program, a filter is designed for the generation of a vibration signal, and the filtered results are approximated with the vibration PSD given by ESA. Through the simulation analysis, the vibration signal is added to the beaconless acquisition simulation program, the vibration amplitude is from -10.7 μrad to 5.9 μrad, when the overlap factor is selected as 10%, it does not produce any leakage scanning area. This method of filtering also has a universal applicability and can be used to analyze the PSD of various satellite platforms in the beaconless acquisition program. Finally, in view of the scope that the scanning scope of the galvanometer cannot cover the whole UC, the sub-regional scanning mode is selected. When the scanning scope of the galvanometer is 1.6 mrad, the sub-regional of $7 * 7$ can completely cover the whole UC. The scanning time is 17.86 s. Through the actual measurement, the acquisition time is 18.21 s, the tracking error are better than 0.4 urad.

References

[1] S. Lambert and W. Casey, "Laser communications in space," *Opt. Eng.*, 1996.
[2] U. Sterr, L. Friederichs, and W. Diebold, "Modelling and analysis of flight dynamics influences on the spatial acquisition and tracking performance of the TESAT laser communication terminal," in *Proc. IEEE Int. Conf. Space Opt. Syst. Appl.*, 2015, pp. 1–5.
[3] F. Heine and S. Seel, "LCT for the European data relay system: In orbit commissioning of the Alphasat and Sentinel 1A LCTs," *Proc. SPIE*, vol. 9354, 2015, Art. no. 93540G.
[4] M. Toyoshima and K. Araki, "In-orbit measurements of short term attitude and vibrational environment on the engineering test satellite VI using laser communication equipment," *Opt. Eng.*, vol. 40, no. 5, pp. 827–832, 2001.
[5] X. Ma, "Spatial acquisition scheme with ultrawide FOV for atmospheric optical links: Based on a fish-eye lens and a sinusoidal amplitude grating," *Appl. Opt.*, vol. 54, no. 13, pp. 4135–4146, 2015.
[6] X. L. Ma, L. Liu, B. Tu, X. Zhang, Z. Zhang, and J. Tang, "Wide-angle lens array spatial acquisition with ultrawide field of view in optical links under atmospheric scintillation and background radiation," *J. Lightw. Technol.*, vol. 28, no. 24, pp. 3582–3588, Dec. 2010.
[7] S. Bai, J. Qiang, and L. Zhang, "Optimization of spatial acquisition systems for low-light-level robustness in space optical communications," *Opt. Lett.*, vol. 40, no. 16, pp. 3750–3753, 2015.
[8] J. Sudey and J. R. Sculman, "In-orbit measurements of Landsat-4 thematic mapper dynamic disturbances," *Acta Astron.*, vol. 12, no. 7/8, pp. 485–503, 1985.
[9] L. Friederichs, U. Sterr, and D. Dallmann, "Vibration influence on hit probability during beaconless spatial acquisition," *J. Lightw. Technol.*, vol. 34, no. 10, pp. 2500–2509, May 2016.
[10] T. Luo and Y. Hu, "Vibration suppression techniques for optical inter-satellite communications," in *Proc. IEEE Int. Conf. Commun.*, 2002, vol. 1, pp. 585–589.
[11] K. I. Schultz and S. Fisher, "Ground-based laser radar measurements of satellite vibrations," *Appl. Opt.*, vol. 31, no. 36, pp. 7690–7695, 1992.
[12] S. Arnon, S. R. Rotman, and N. S. Kopeika, "Performance limitations of a free-space optical communication satellite network owing to vibrations: Heterodyne detection," *Appl. Opt.*, vol. 37, no. 27, pp. 6366–6374, 1998.
[13] Q. Wang, L. Y. Tan, and J. Ma, "A novel approach for simulating the optical misalignment caused by satellite platform vibration in the ground test of satellite optical communication systems," *Opt. Exp.*, vol. 20, no. 2, pp. 1033–1045, 2012.
[14] J. Wang, J. Lv, and G. Zhao, "Free-space laser communication system with rapid acquisition based on astronomical telescopes," *Opt. Exp.*, vol. 23, no. 16, pp. 20655–20667, 2015.
[15] J. Wang, J. M. Kahn, and K. Y. Lau, "Minimization of acquisition time in short-range free-space optical communication," *Opt. Commun.*, vol. 41, no. 36, pp. 20655–20667, 2015.
[16] Q. Wang, Y. Liu, and J. Ma, "Quick acquisition and recognition method for the beacon in deep space optical communications," *Appl. Opt.*, vol. 55, no. 34, pp. 9738–9743, 2016.

[17] S. Arnon, "Use of satellite natural vibrations to improve performance of free-space satellite laser communication," *Appl. Opt.*, vol. 37, no. 21, pp. 5031–5038, 1998.
[18] M. Wittig, L. Holtz, and D. Tunbridge, "In-orbit measurements of microaccelerations of ESA's communication satellite OLYMPUS," *Proc. SPIE*, vol. 1218, 2015.
[19] G. Picchi, G. Prati, and D. Santerini, "Algorithms for spatial laser beacon acquisition," *IEEE Trans. Aerosp. Electron. Syst.*, vol. AES-22, no. 2, pp. 106–114, Mar. 1986.
[20] D. Dallmann, M. Reinhardt, M. Gregory, F. Heine, U. Sterr, and R. Meyer, "GEO-LEO beaconless spatial acquisition reality in space," in *Proc. IEEE Int. Conf. Space Opt. Syst. Appl.*, 2015.
[21] B. Tu, L. Liu, and Y. Liu, "Acquisition probability analysis of ultra-wide FOV acquisition scheme in optical links under impact of atmospheric turbulence," *Appl. Opt.*, vol. 52, no. 14, pp. 3147–3155, 2013.
[22] X. Li, S. Yu, and J. Ma, "Analytical expression and optimization of spatial acquisition for intersatellite optical communications," *Opt. Exp.*, vol. 52, no. 14, pp. 3147–3155, 2011.
[23] T. Mendenhall and M. Narigon, "Satellite optical communication beam acquisition techniques," U.S. Patent 6 535 314 B1, Mar. 18, 2003.
[24] U. Sterr, M. Gregory, and F. Heine, "Beaconless acquisition for ISL and SGL, summary of 3 years operation in space and on ground," in *Proc. IEEE Int. Conf. Space Opt. Syst. Appl.*, 2011, pp. 38–43.
[25] C.-Y. Li and W.-S. Tsa, "A 150m/22.5 Gbaud PAM4-based FSO link," *Laser Phys. Lett.*, vol. 14, no. 6, 2017, Art. no. 065202.
[26] S. Yu, F. Wu, and Q. Wang, "Theoretical analysis and experimental study of constraint boundary conditions for acquiring the beacon in satellite-ground laser communications," *Opt. Commun.*, vol. 40, no. 2, pp. 585–592, 2017.